Phenomenological rate formulas for over-barrier ionization of hydrogen and helium atoms in strong constant electric fields

Svea Remme, Alexander Voitkiv, Georg Pretzler, Carsten Müller

Journal of Physics B:
Atomic, Molecular and
Optical Physics

PAPER • **OPEN ACCESS**

Phenomenological rate formulas for over-barrier ionization of hydrogen and helium atoms in strong constant electric fields

To cite this article: S Remme *et al* 2025 *J. Phys. B: At. Mol. Opt. Phys.* **58** 195602

OPEN ACCESS
IOP Publishing
Journal of Physics B: Atomic, Molecular and Optical Physics
J. Phys. B: At. Mol. Opt. Phys. **58** (2025) 195602 (10pp)
https://doi.org/10.1088/1361-6455/ae0540

Phenomenological rate formulas for over-barrier ionization of hydrogen and helium atoms in strong constant electric fields

S Remme[1], A B Voitkiv[1], G Pretzler[2] and C Müller[1,*]

[1] Institut für Theoretische Physik I, Heinrich-Heine-Universität Düsseldorf, 40225 Düsseldorf, Germany
[2] Institut für Laser- und Plasmaphysik, Heinrich-Heine-Universität Düsseldorf, 40225 Düsseldorf, Germany

E-mail: c.mueller@tp1.hhu.de

Received 6 June 2025, revised 25 August 2025
Accepted for publication 8 September 2025
Published 7 October 2025

Abstract

Nonrelativistic over-barrier ionization (OBI) of atoms in strong constant electric fields is studied, focussing on hydrogen and helium as concrete examples. Our goal is, on the one hand, to develop an intuitive physical picture behind established empirical formulas for the ionization rate. We show that the ionization rate in a near OBI regime can be modeled quantitatively by extending corresponding tunneling rates by the combined action of the Stark effect and a widened electron emission angle. On the other hand, we present analytical rate formulas in a far OBI regime which closely agree with available numerical data. In result, compact rate expressions describing OBI of hydrogen-like and helium atoms in a broad range of applied field strengths are obtained. They can be useful, for example, in numerical laser-plasma simulation codes to describe elementary ionization events.

Keywords: over-barrier ionization, strong electric fields, Stark effect

1. Introduction

Ionization of atoms in strong electric fields is a fundamental process of relevance in various areas of physics [1]. It constitutes, e.g. the starting point for high-harmonic and attosecond pulse generation [2] or advanced concepts of laser-plasma acceleration [3]. Strong-field ionization is also of interest from a basic physical perspective because, when the field is static or slowly varying, the ionization possesses a manifestly nonperturbative character: its rate depends exponentially on the inverse of the field strength. This renders strong-field ionization an important process to study nonperturbative physics in a quantum system.

As long as the applied field strength remains far below a certain threshold value, $F \ll F_c$, the ionization proceeds as a quantum tunneling process, where the electron escapes from the atom through the potential barrier that is formed by the superposition of the binding Coulomb potential and the applied external potential. Ionization in the tunneling regime is a well-understood phenomenon and accurately described by the quasiclassical Ammosov–Delone–Krainov (ADK) [4] (or Perelomov–Popov–Terent'ev [5]) theory.

However, when the field amplitude exceeds the critical value F_c, the maximum of the deformed potential lies below the atomic binding energy and the electron may leave the atom above the barrier without the need to tunnel. The process then goes over from tunneling to over-barrier ionization (OBI). As a consequence, for $F \gtrsim F_c$, the ADK tunneling rate looses

* Author to whom any correspondence should be addressed.

its applicability and substantially overestimates the ionization yield [6–10].

While ionization rates in the tunneling regime have been derived in analytical form, the OBI is more difficult to treat theoretically. Early analytical attempts [11, 12] did not provide convincing results, as was shown in [6] by comparison with 'exact' OBI rates obtained from solving the three-dimensional time-dependent Schrödinger equation numerically in a wide range of applied field strengths. Apart from the possibility of fully numerical approaches [6–9, 13], also compact empirical rate formulas for OBI in constant electric fields exist [8, 14] that represent extensions of the ADK tunneling rate. They have been obtained by parameter fits to numerical ionization data and achieve very good agreement for field strengths up to a few times the critical value. A drawback of these successful empirical expressions is, however, that they lack a physical explanation or motivation for their functional form. It is one of the goals of the present paper to fill this gap by proposing a physically intuitive interpretation of these rate formulas in the near OBI regime.

The second goal of our paper is to present compact analytical formulas for the ionization rate in the far OBI regime, where the applied field strength $F \gg F_\mathrm{c}$ approaches or even exceeds the atomic field strength F_a. On the one hand, a quadratic dependence of the rate on the applied field has been found around $F \sim 0.3F_\mathrm{a}$ as an approximate fit to numerical data [6], whereas on the other hand, a linear field dependence has been predicted for $F \gtrsim F_\mathrm{a}$ by a so-called motionless approximation [15]. We will obtain a unified formula that is applicable for a broad range of field strengths and that is in good agreement with the available numerical data for hydrogen [6] and helium [7] in the far OBI regime. This formula can also be joined with analytical expressions valid in the near OBI regime, so that the full OBI range is covered.

Our consideration is restricted to the nonrelativistic domain. We point out that, very recently, a comprehensive theory for relativistic strong-field ionization including OBI has been developed [16]. It relies on an adiabatic approximation for the transition amplitude and applies generalized eikonal theory to describe the electron states. The ionization rate is then obtained by numerical evaluation of the corresponding amplitude.

The present paper is organized as follows. In section 2 we describe our approach to strong-field ionization in the near-OBI regime where $F \gtrsim F_\mathrm{c}$. It relies on physically motivated modifications to the ADK tunneling rate, resulting from inclusion of the Stark effect and accounting for a widened range of electron emission angles. The corresponding predictions will be compared with established empirical OBI rate formulas [8, 14] and fully numerical data for hydrogen [6, 17, 18] and helium [7]. Afterwards, the far-OBI regime of field strengths $F \gg F_\mathrm{c}$ is considered in section 3, where a novel fit formula is introduced that contains previously determined scaling laws [6, 15] approximately as limiting cases. Finally, our results in the near-OBI and far-OBI regimes are combined to provide compact empirical rate expressions for hydrogen and helium applicable in a broad range of field strengths. Section 4 addresses some aspects beyond atomic physics. The conclusions from our considerations are given in section 5.

Atomic units (a.u.) are used throughout unless explicitly stated otherwise. We note that one atomic unit of electric field strength corresponds to 5.14×10^9 V cm^{-1}.

2. Ionization in the near-OBI regime

We consider ionization in a constant electric field F, pointing in negative z direction. The corresponding interaction potential with the atomic electron reads $\hat{V} = -Fz$. The ADK formula of tunneling ionization has been derived for a general bound state with binding energy $-I_\mathrm{p}$ and angular momentum quantum numbers ℓ and m [4, 19]. However, for our purposes it is sufficient to consider the special case of a $1s$ ground state, where the ADK formula reduces to [8, 19]

$$W_\mathrm{TI}(F,\kappa) = \frac{C_\mathrm{a}^2}{2\kappa^{2Z_\mathrm{c}/\kappa-1}}\left(\frac{2\kappa^3}{F}\right)^{2Z_\mathrm{c}/\kappa-1}\exp\left(-\frac{2\kappa^3}{3F}\right), \quad (1)$$

with $\kappa = \sqrt{2I_\mathrm{p}}$, the charge Z_c of the atomic core, and an atom-specific parameter C_a that reads $C_\mathrm{a} = 2\kappa^{3/2}$ for hydrogen-like systems. The rate W_TI features a characteristic dependence on $1/F$ in the exponential, which gives the rate a manifestly nonperturbative nature. Equation (1) applies for field strengths $F \ll F_\mathrm{c}$ far below the critical value

$$F_\mathrm{c} = \frac{I_\mathrm{p}^2}{4Z_\mathrm{c}}, \quad (2)$$

where the Coulomb potential is suppressed all the way down to the (unperturbed) bound-state energy level [20]. For hydrogen-like systems, the critical field can also be written as $F_\mathrm{c} = \kappa^3/16$, since $\kappa = Z_\mathrm{c}$ holds in this case.

When the field is not too large ($F \lesssim 4F_\mathrm{c}$), it is in principle possible to take the ADK tunneling formula as basis and modify it by suitable correction factors. By fitting to numerical ionization rates that have been obtained by the complex scaling method, Tong and Lin have proposed the following empirical OBI rate formula [8]:

$$W_\mathrm{OBI}^\mathrm{(TL)}(F,\kappa) = W_\mathrm{TI}(F,\kappa)\exp\left(-\alpha\frac{Z_\mathrm{c}^2}{I_\mathrm{p}}\frac{F}{\kappa^3}\right), \quad (3)$$

with a single, atom-specific fit parameter α. The latter has been determined for a number of atomic species in [8]. In particular, taking $Z_\mathrm{c} = 1$ and $\alpha = 6$ for hydrogen, this formula works well up to $F \approx 2.5F_\mathrm{c}$. The correction factor depends on the properties of the considered atom and scales in the exponent linearly with the applied field.

By the same strategy, a three-parameter correction factor was obtained by Zhang *et al* [14, 21]:

$$W_\mathrm{OBI}^\mathrm{(ZLL)}(F) = W_\mathrm{TI}(F,\kappa)\exp\left(a_1\frac{F^2}{F_\mathrm{c}^2} + a_2\frac{F}{F_\mathrm{c}} + a_3\right). \quad (4)$$

In addition to a linear term $\sim F$ in the exponent of the correction factor, it also contains a constant and a quadratic term $\sim F^2$. The enlarged number of fit parameters allows the

authors to extend the applicability range of their OBI rate formula as compared with equation (3). For the case of hydrogen, equation (4) gives good results up to $F \approx 4.5F_c$, with the optimized values $a_1 = 0.11714$, $a_2 = -0.90933$ and $a_3 = -0.06034$.

While both empirical formulas (3) and (4) agree well with numerically determined ionization rates, their drawback is to not provide a physical explanation for the functional form of the correction factors. In the following we present an intuitive, physically motivated procedure to obtain ionization rates in the near OBI regime by suitable modifications/extensions of the ADK formula (1). Our approach relies on the inclusion of the Stark effect in both the bound-state energy and bound-state wave function along with a geometrically inspired rate averaging over the electron emission angles.

2.1. Inclusion of Stark effect in binding energy

The ADK theory relies on the assumption that the initial bound state remains unaltered in the presence of the external field. While this is justified for $F \ll F_c$, higher fields exert a sizeable influence on the bound electron by the Stark effect [10, 16, 22–24]. In our treatment of near OBI we account for the Stark effect in the lowest (i.e. second) order of perturbation theory. The resulting shift of the binding energy in the $1s$ ground state of hydrogen reads

$$\varepsilon_S^{(2)} = \sum_{n>1} \frac{\left|\langle\psi_{n10}^{(0)}|\hat{V}|\psi_{100}^{(0)}\rangle\right|^2}{\varepsilon_1 - \varepsilon_n} + \int \mathrm{d}^3p \, \frac{\left|\langle\psi_{\vec{p}}^{(0)}|\hat{V}|\psi_{100}^{(0)}\rangle\right|^2}{\varepsilon_1 - \varepsilon_p}. \quad (5)$$

Here, $\psi_{n\ell m}^{(0)}$ denotes the unperturbed bound state with quantum numbers n, ℓ, m and energy ε_n, whereas $\psi_{\vec{p}}^{(0)}$ is an unperturbed Coulomb wave with asymptotic momentum $\vec{p}$ and energy $\varepsilon_p = \frac{p^2}{2}$. The Stark shift energy in this case is known exactly; it is quadratic in the applied field and amounts to [25]

$$\varepsilon_S^{(2)} = -I_S \;\text{ with }\; I_S = \frac{9}{4}\frac{F^2}{\kappa^4}\,. \quad (6)$$

One can already see here that the Stark shift leads to stronger binding of the ground state electron and, thus, to reduced ionization. As a side remark we note that by far the largest contribution to I_S stems from the $2p_0$ state in equation (5) with almost 66%; the rest comes in roughly equal shares from the higher lying bound states ($n \geqslant 3$) and the continuum states, respectively. The second-order perturbative prediction for the Stark shift (6) may be considered a reasonably good approximation up to field strengths $F \sim 0.1$ a.u. ($\approx 1.5F_c$), where it underestimates the exact result by less than 25%, according to the complex-scaling calculations in [17, 18].

To extend the ADK rate formula into the near OBI regime, our first modification will be to replace the binding potential I_p by $I_p + I_S$ in equation (1), both in the preexponential factor and the exponential. It is interesting to note that, by performing a Taylor expansion $(I_p + I_S)^{3/2} \approx I_p^{3/2} + \frac{3}{2} I_S I_p^{1/2}$ in the exponential of the resulting rate expression for $I_S \ll I_p$, one obtains

$$\mathrm{e}^{-\frac{2\kappa^3}{3F}} \to \mathrm{e}^{-\frac{2\kappa^3}{3F}} \exp\left(-\frac{9}{2}\frac{F}{\kappa^3}\right). \quad (7)$$

By comparison with equation (3) we see that the exponential correction factor to the tunneling rate that results from inclusion of the (quadratic) Stark energy shift, has the same structure as the Tong–Lin factor, showing a linear dependence on F. The numerical prefactor amounts to $3/8$ of the corresponding prefactor in equation (3), which yields $W_{\mathrm{OBI}}^{(\mathrm{TL})}/W_{\mathrm{TI}} = \exp(-12F/\kappa^3)$ for hydrogen. Thus, one may infer that a good portion of the correction factor of Tong and Lin can be associated with the Stark shift of the bound-state energy. For comparison we note that a factor of approx. -5 instead of $-9/2$ in the exponent has been obtained by an adiabatic-eikonal treatment of strong-field ionization, where the Stark effect is included beyond perturbation theory (see section 3.2 in [16]).

It is worth noting at this point that the Stark effect has been included in the ADK tunneling rate to explain angular asymmetries arising in the strong-field ionization of oriented heteroatomic molecules [22, 23]. In this situation, also a linear Stark shift $\varepsilon_S^{(1)}$ occurs, since the considered hydrogen chloride (HCl) and carbonylsulphide (OCS) molecules possess permanent dipole moments. Depending on the relative orientation of the molecular axis to the applied field, the linear Stark shift either lowers or increases the ionization potential. This leads to correspondingly enhanced or reduced ionization yields, i.e. to orientation-dependent asymmetries in the angular distributions of emitted photoelectrons. Also the quadratic Stark shift $\varepsilon_S^{(2)}$ was accounted for in the analysis of the experimental results [22, 23].

While one might speculate that an observation like in equation (7) has motivated the form of the correction factor assumed by Tong and Lin, a link to the Stark effect is not mentioned in their paper [8]. Moreover, to the best of our knowledge, this connection has so far remained unnoticed in the literature. Being aware of it is important because sometimes the Stark shift up to second order is inserted via $I_p \to I_p - (\varepsilon_S^{(1)} + \varepsilon_S^{(2)})$ into the Tong–Lin formula [26]. However, this can lead to a double counting of the quadratic Stark effect, because the Tong–Lin formula already contains this effect, according to the interpretation that equation (7) suggests.

2.2. Inclusion of Stark effect in bound-state normalization

The Stark effect also affects the wave function $\psi_{100}^{(0)}$ of the bound state, leading to a polarization of the atom along the field direction. Two contributions to the atomic polarization can be distinguished [16]: (i) the shift of the bound electron state towards the 'tunnel exit'. This effect, which leads to *enhanced* ionization, is implicitly accounted for in the ADK formula by a corresponding shift of the matching point between the unperturbed bound state and the continuum state of the electron [4, 19, 25]. Within the generalized eikonal approach of [16] it manifests in a coordinate-dependent

correction factor to the unperturbed bound state. Conversely, (ii) the bound state distortion constitutes a global, coordinate-independent correction to the wave-function normalization constant [16], that causes a *reduction* of the ionization rate. Since the ADK rate does not include this effect, it needs to be modified in our treatment by a corresponding correction factor in the OBI regime. Below we shall argue how an approximate version of such a correction factor may be obtained within perturbation theory.

The first-order correction of the unperturbed ground state is given by

$$\psi_{100}^{(1)} = \sum_{n>1} \frac{\langle \psi_{n10}^{(0)} | \hat{V} | \psi_{100}^{(0)} \rangle}{\varepsilon_1 - \varepsilon_n} \psi_{n10}^{(0)} + \int \mathrm{d}^3 p \, \frac{\langle \psi_{\vec{p}}^{(0)} | \hat{V} | \psi_{100}^{(0)} \rangle}{\varepsilon_1 - \varepsilon_p} \psi_{\vec{p}}^{(0)}$$

and, thus, orthogonal to the unperturbed ground state. In contrast, the second-order correction $\psi_{100}^{(2)}$ contains a contribution proportional to $\psi_{100}^{(0)}$, leading to a non-zero overlap $\langle \psi_{100}^{(2)} | \psi_{100}^{(0)} \rangle = -\frac{1}{2}\beta F^2$ with [25]

$$\beta = \sum_{n>1} \left| \frac{\langle \psi_{n10}^{(0)} | \hat{z} | \psi_{100}^{(0)} \rangle}{\varepsilon_1 - \varepsilon_n} \right|^2 + \int \mathrm{d}^3 p \left| \frac{\langle \psi_{\vec{p}}^{(0)} | \hat{z} | \psi_{100}^{(0)} \rangle}{\varepsilon_1 - \varepsilon_p} \right|^2 . \tag{8}$$

The numerical value of this parameter turns out as $\beta \approx 4.912$. The correspondingly perturbed state $\psi_{100} = \psi_{100}^{(0)} + \psi_{100}^{(1)} + \psi_{100}^{(2)}$ (that is normalized up to order $\mathcal{O}(F^2)$) hence contains the portion $\psi_{100} = N\psi_{100}^{(0)} + \ldots$ proportional to the unperturbed ground state, where

$$N = 1 - \frac{\beta}{2} F^2 \tag{9}$$

represents an adjusted 'normalization constant' for the $\psi_{100}^{(0)}$ contribution. Our second modification of the ADK formula due to the Stark effect shall be to multiply equation (1) by $|N|^2 \approx 1 - \beta F^2$, since the ground state $\psi_{100}^{(0)}$ enters quadratically in the ADK ionization rate.

We emphasize that all the other contributions to the perturbed ground state ψ_{100} are dropped in our consideration. Essentially, this simplifying step can only be justified *a posteriori* by a remarkably good agreement of the predictions from our phenomenological treatment with accurate numerical ionization rates (see section 3). Additionally, it might be argued that the contributions from the excited bound and continuum states to ψ_{100} are mainly responsible for the polarization shift of the ground state, which is already contained in the ADK rate.

The modified normalization constant (9) may be interpreted as reflecting (part of) the distortion of the initial-state wave function by the Stark effect. For comparison we note that in section 3.2 of [16], a corrected normalization constant of $1 - \frac{31}{4}F^2$ has been found, which possesses the same structure as equation (9). In line with the results of this recent study, both the Stark shift of the binding energy (6) and the Stark distortion of the wave function (9) lead to reductions of the ionization rate.

The alteration of the state normalization can be linked, at least qualitatively, to the appearance of a quadratic term in the correction factor of Zhang *et al* in equation (4) because, provided that $\beta F^2 \ll 1$ holds, one may write approximately $|N|^2 \approx \exp\left(-\beta F^2\right)$.

We conclude sections 2.1 and 2.2 by noting that an asymptotic perturbative expansion of the ionization rate for hydrogen in powers of the field has obtained a correction factor up to quadratic order of $1 - \frac{53}{12}F - \frac{3221}{8\cdot 36}F^2$ [27]. We note that the numerical factor in the linear term is very close to the $9/2$ in equation (7). An extension of this weak-field asymptotic theory has been provided via Siegert states [24]; the corresponding results are applicable to a larger class of atoms and field strengths approaching the boundary between tunneling and OBI.

2.3. Accounting for widened range of emission angles

With the two Stark-effect modifications from section 2.1 and 2.2 included, our preliminary expression for the ionization rate in the near OBI regime reads

$$\tilde{W}_{\mathrm{nOBI}}(F, \kappa') = |N|^2 \, W_{\mathrm{TI}}(F, \kappa') \tag{10}$$

with $\kappa' = \sqrt{2(I_\mathrm{p} + I_S)}$. The final modification that we are going to carry out to the ADK formula (1) is geometrically motivated. In a tunneling description, the electron leaves the atom—essentially—along the z direction, i.e. opposite to the applied field [19, 25]. This is reasonable because in this direction the tunnel is shortest and the potential barrier lowest. The other emission directions are subject to even stronger exponential suppressions and may therefore be neglected. Conversely, in the OBI regime, the 'door is open' for the electron since the potential is suppressed completely. This holds not only for the direction along the field axis, but for a range of emission angles, as is illustrated in figure 1.

We can determine the maximum angle $\vartheta_{\max}$ under which the electron can leave the atom above the barrier from the total potential $\hat{V}_{\mathrm{tot}}(r, \vartheta) = -Fr\cos\vartheta - \frac{\kappa}{r}$ by demanding that its maximum value with respect to the radial coordinate equals the Stark-shifted ground-state energy. This leads to the relation $2\sqrt{\kappa F \cos\vartheta_{\max}} = I_\mathrm{p} + I_S$, from which

$$\vartheta_{\max} = \arccos\left[\frac{F_\mathrm{c}}{F}\left(1 + \frac{I_S}{I_\mathrm{p}}\right)^2\right] \tag{11}$$

follows. Thus, when emitted within a cone of opening angle $\vartheta_{\max}$ around the z axis (about which the problem is symmetric), the electron is ionized above the barrier. Since the emission directions within this cone are not suppressed by the need to tunnel, all of them may contribute to ionization. The electron thus has a 'free choice' of pathways and since one does not know which way it goes, it appears reasonable to take an average over the relevant range of emission angles, according to

$$W_{\mathrm{nOBI}}(F, \kappa) = \frac{1}{\vartheta_{\max}} \int_0^{\vartheta_{\max}} \tilde{W}_{\mathrm{nOBI}}(F\cos\vartheta, \kappa') \, \mathrm{d}\vartheta \, . \tag{12}$$

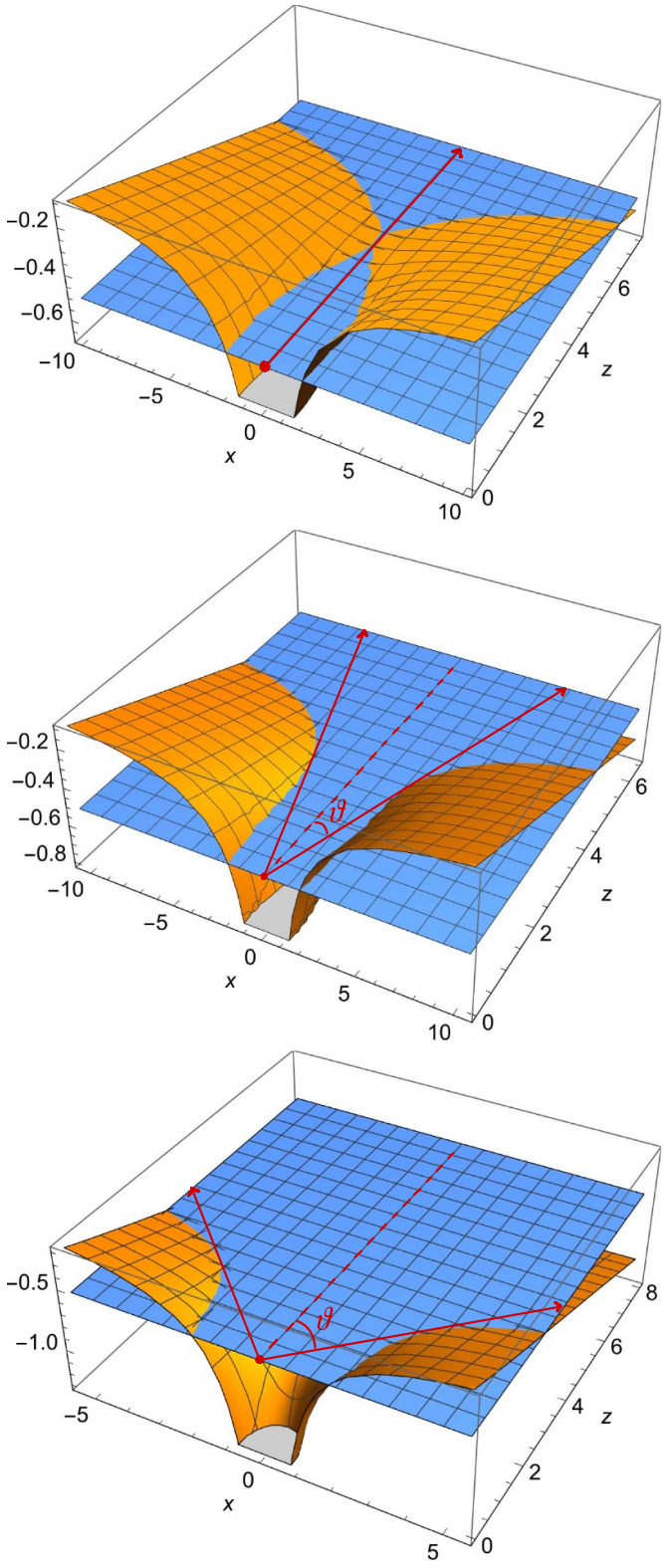

Figure 1. Total potential $\hat{V}_{\rm tot} = -Fr\cos\vartheta - \frac{1}{r}$, consisting of the external field potential and the atomic Coulomb potential of hydrogen (curved orange plane). The horizontal plane in blue indicates the location of the Stark-shifted bound-state energy $-(I_{\rm p} + I_S)$. The external field is taken as $F = 1.04F_c$ in the top panel, $F = 1.5F_{\rm c}$ in the middle panel, and $F = 2F_{\rm c}$ in the bottom panel.

This angular averaging can be applied for field strengths $F \geqslant F_{\rm min}$ which are large enough, so that the argument of the arccosine in equation (11) is $\leqslant 1$. The corresponding atom-specific threshold field $F_{\rm min}$ lies slightly above $F_{\rm c}$ (e.g. $F_{\rm min} = 1.04F_{\rm c}$ for hydrogen). The integral in equation (12) is evaluated numerically.

We note that the maximal opening angle $\vartheta_{\rm max}$ goes to zero when the applied field strength approaches to $F_{\rm min}$ from above. In this limit, the integrand in equation (12) is approximately constant and the equation goes over to $W_{\rm nOBI}(F,\kappa) = \tilde{W}_{\rm nOBI}(F,\kappa')$, so that a smooth transition towards smaller fields $F < F_{\rm min}$ is guaranteed.

In order to properly interpret the angular average in equation (12) it is worth recalling that, in the derivation of the ADK formula (1), the z-component of the electron current density—which lies antiparallel to the field direction—is transformed into an ionization rate by an area integral over a transverse plane [19, 25]. Accordingly, since the modified tunneling rates $\tilde{W}_{\rm nOBI}(F\cos\vartheta,\kappa')$ on the right-hand side of equation (12) rely on equation (1), they contain this area integration. However, instead of an electron flux in z-direction (corresponding to $\vartheta = 0$), they refer to electron emission under the angle ϑ which may vary from zero up to $\vartheta_{\rm max}$. In this way, a broader range of electron emission directions is taken into account.

2.4. Near-OBI results for hydrogen and helium

In the following we will compare the predictions from our rate formulas (10) and (12), including the Stark effect and the widened emission range, with other empirical rates [8, 14] and with fully numerical results [7, 18].

2.4.1. Near-OBI of hydrogen and hydrogen-like ions.

Figure 2 shows the ionization rate of hydrogen in a near-OBI regime around the critical field strength $F_{\rm c}$. The ADK tunneling rate (1), shown by the dotted blue curve, is seen to significantly overestimate the ionization. Our rate prediction (solid black line) lies slightly above the empirical rates (3) and (4), which agree well with the 'exact' rate resulting from fully numerical complex-scaling calculations [18]. The difference between our result and these other predictions is largest close to $F \approx F_{\rm c}$; it starts to improve significantly when the angular averaging is included for $F \geqslant 1.04F_{\rm c}$. For the highest field strengths shown in the figure, our rate reaches close agreement with the predictions from equations (3), (4) and [18]. The figure also shows by the dash-triple-dotted red line an analytical approximation from [16], based on equation (A2) therein for the ionization amplitude (including a factor $\frac{1}{2}$); at higher field values, the corresponding rate lies slightly above the other OBI predictions.

Figure 3 focusses on the near-OBI regime above F_c. It shows the empirical rate (4) as a (dash-dotted purple) reference line, since the numerical results of [18] are restricted to $F \leqslant 0.1$ a.u. $\approx 1.5F_{\rm c}$. When the ADK tunneling rate $W_{\rm TI}(F,\kappa)$

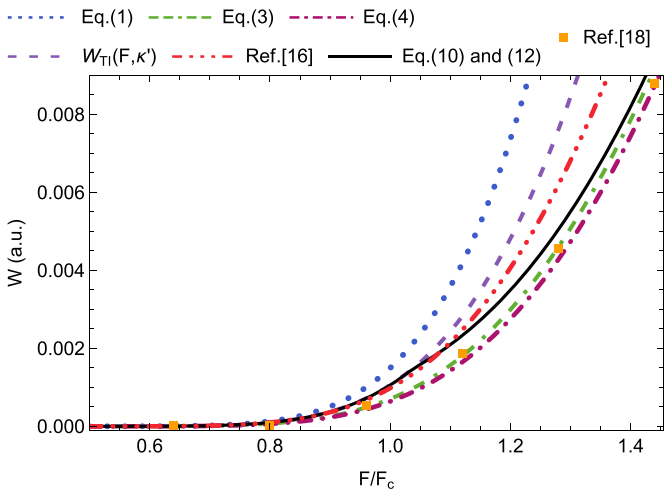

Figure 2. Ionization rates for atomic hydrogen from the ground state in a near-OBI regime of field strengths around F_c. The dotted blue line shows the ADK tunneling rate (1), while the short-dashed violet line includes the rate modification from the Stark-shifted binding energy. The solid black line shows our equation (10) for $F \leqslant 1.04F_c$ and our equation (12) for $F \geqslant 1.04F_c$, with the latter involving the angular averaging. The dash-dotted purple line is the empirical formula (4) by Zhang *et al* [14], the double-dash-dotted green line the empirical formula (3) by Tong and Lin [8], and the dash-triple-dotted red line is based on equation (A2) of Klaiber *et al* [16]. The orange squares are numerical results by Maltsev *et al* [18].

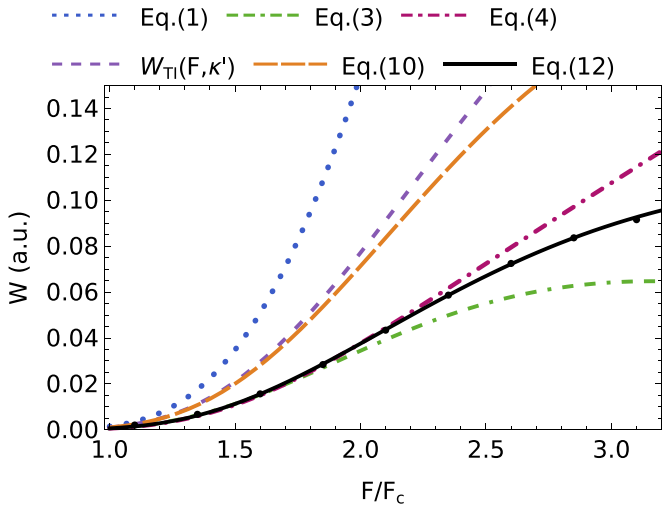

Figure 3. Ionization rates for atomic hydrogen from the ground state in a near-OBI regime of field strengths above F_c. The dotted blue line shows the prediction of the ADK tunneling rate (1), the short-dashed violet line includes the rate modification from the Stark-shifted binding energy, the long-dashed orange line includes in addition the Stark-modification of the wave-function normalization, and the black marker points show the results from equation (12). The solid black line connecting the marker points shows the fit formula (13). The dash-dotted purple line results from the empirical formula (4), whereas the double-dash-dotted green line shows the empirical formula (3).

(dotted blue line) is amended to $W_{TI}(F,\kappa')$ by inclusion of the Stark energy shift, the short-dashed violet curve results. It lies already much closer to the reference rate. Additional account of the Stark effect in the wave function normalization leads to a further approach, as the long-dashed orange line displays. Inclusion of the widened angular emission range according to equation (12) finally leads to very good agreement between our rate prediction (black marker points) with the empirical rate (4) by Zhang *et al* up to field strengths $F \approx 2.5F_c$. The black solid line in figure 3 was obtained as an analytical fit of the form (see also equation (4))

$$W_{\mathrm{nOBI}}^{(\mathrm{fit})} = W_{\mathrm{TI}}(F,\kappa)\exp\left(\tilde{a}_1\frac{F^2}{F_c^2}+\tilde{a}_2\frac{F}{F_c}+\tilde{a}_3\right) \tag{13}$$

to our results from equation (12). The values of the fit parameters that we obtained, are given in table 1. We may thus conclude that our rate formula (12), that was obtained by physically motivated modifications to the ADK tunneling rate, has a similar range of applicability for OBI of hydrogen as the empirical rate (3) by Tong and Lin. We note that, interestingly, the upper boundary of the applicability range of about $2.5F_c \approx 0.16$ a.u. lies close to the alternative value of 0.146 a.u. of the critical OBI field for hydrogen obtained in [20]. This coincidence might explain why the ionization rate in this regime can be described by modified tunneling-like formulas. We furthermore note that, in the limit of low fields $F \ll F_c$, the modified rate formula in equation (13) approximately goes over to the ADK tunneling rate $W_{\mathrm{TI}}(F,\kappa)$, because the absolute value of the fit parameter $\tilde{a}_3$ is small, $|\tilde{a}_3| \ll 1$.

Table 1. Optimized parameters to fit the near-OBI rate from equation (12) to the analytical form (13).

	$\tilde{a}_1$	$\tilde{a}_2$	$\tilde{a}_3$
Hydrogen	0.047 769	−0.745 282	−0.114 022
Helium	0.042 177	−0.762 430	0.039 149

Our results for hydrogen carry over to OBI of hydrogen-like ions with nuclear charge Z by virtue of a scaling transformation. The rate for ionization of an ion with charge Z in a field of strength F is obtained from the rate for ionization of hydrogen by evaluating the latter at the scaled field F/Z^3 and multiplying the result with Z^2. Since our treatment is nonrelativistic, the nuclear charge is restricted to values of about $Z \lesssim 20$ where relativistic effects in the ion may be neglected.

2.4.2. Near-OBI of helium. By some suitable adjustments, we can apply our empirical approach also to OBI of helium. A comparison of corresponding near-OBI rates obtained by different methods is shown in figures 4 and 5. Since the helium ground state contains two 1*s* electrons, the ADK rate has been multiplied by a factor of 2 and the atom-specific parameter in equation (1) set to $C_a = 2.67$ [4, 28]. The critical field in case of helium amounts to $F_c = 0.204$ a.u. by virtue of equation (2), with the charge $Z_c = 1$ of the atomic core.

In order to catch the main physical properties of helium within our effective one-electron model, we shall use effective nuclear charges. Into the ADK tunneling rate (1), the binding potential $I_p = 0.904$ a.u. enters, corresponding to $\kappa \approx 1.345$. To estimate the Stark effect in helium, we use an effective

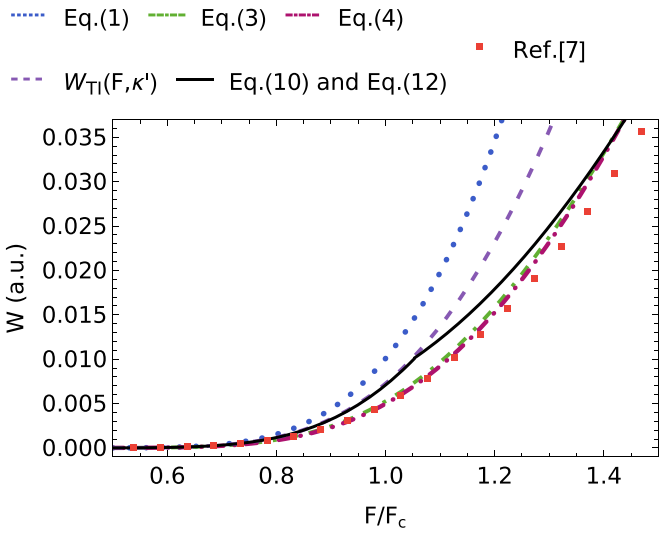

Figure 4. Ionization rates for helium from the ground state in a near-OBI regime of field strengths around F_c. The dotted blue line, short-dashed violet line, solid black line, dash-dotted purple line and double-dash-dotted green line have the equivalent meanings as in figure 2. The transition from equations (10)–(12) along the black line occurs here at $F = 1.05F_c$, in accordance with equation (11). The red marker squares are numerical results by Scrinzi *et al* [7].

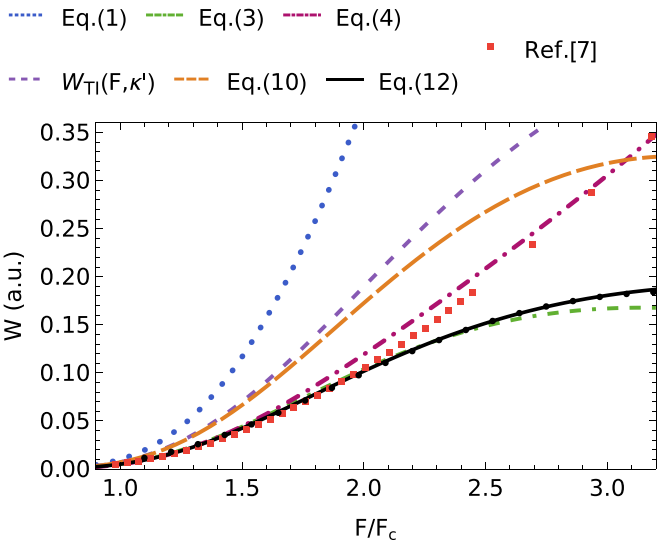

Figure 5. Ionization rates for helium from the ground state in a near-OBI regime of field strengths above $F_c = 0.204$ a.u. The dotted blue line shows the ADK tunneling rate, the short-dashed violet line includes the rate modification from the Stark-shifted binding energy, the long-dashed orange line includes in addition the Stark-modification of the wave-function normalization, and the black marker points show the results from equation (12). The solid black line connecting the marker points shows the fit formula (13). The double-dash-dotted green line is the empirical formula (3) by Tong and Lin [8] (with $\alpha = 7$), the dash-dotted purple line is the empirical formula (4) by Zhang *et al* [14], and the red marker squares are the numerical results by Scrinzi *et al* [7].

nuclear charge $Z_S \approx 1.44$ that results from the $1s$–$2p$ transition energy. Our choice is motivated by the fact, that this transition gives by far the largest contribution to the Stark shift of the binding energy (see the remark below equation (6)). This way, we obtain $I_S \approx 0.523F^2$ [29] from equation (6) and $\beta \approx 0.551$ in the normalization constant (9).

Near-OBI rates for helium in a regime of field strengths around the critical value are displayed in figure 4. As for the case of hydrogen in figure 2, our phenomenological rate prediction (black line) which is composed of equations (10) and (12), lies pretty close to the empirical rate formulas (3) and (4), as well as to the numerical reference points which may be considered as exact ionization rates. The latter have been obtained through fully numerical complex-scaling calculations by Scrinzi *et al* [7]. We note that these numerical rates have recently been confirmed by multiconfiguration time-dependent Hartree–Fock computations [9]. The region of field strengths above F_c is shown in figure 5. It illustrates that, by successively including the Stark shift to the binding energy (short-dashed violet curve), the Stark effect in the wave function normalization (long-dashed orange curve), and the widened emission range (black marker points, connected by solid black line), our rate prediction approaches more and more to the 'exact' ionization rate from [7] up to field strengths of $F \approx 2.05F_c$. Concerning the lower boundary of the applicability range, we note that our fit formula (13) for near-OBI of helium turns out to work well at field strengths of $F \approx 0.5F_c$ already, even though it was obtained by fitting to numerical rates at $F \geqslant F_c$.

Similarly as in the case of hydrogen, our near-OBI rate formula (12) (respectively (13)) performs well up to field strengths of $F \gtrsim 2F_c$. For higher fields, our predictions fall more and more below the numerical results of [7]. Growing deviations in this high-field regime can be expected because of the underlying approximations, e.g. regarding the applied value (6) of the Stark energy shift. However, since this value underestimates the correct Stark shift at high fields and, thus, the binding strength to the atomic core, one would rather expect our formulas to overestimate the numerical OBI rates, which is not the case. For this reason, we interpret the deviations to originate from the more general fact that the nature of the ionization departs more and more from a tunneling-like process when the applied fields become too high. The three-parameter fit formula (4) can resist this trend longer than the empirical one-parameter formula (3) and our phenomenological parameter-free rate (12), but eventually all of them loose their applicability.

3. Ionization of hydrogen and helium in the far-OBI regime

When the external field strength F increases beyond a few times the critical field F_c, the empirical equations (3), (4) and (12) are not applicable anymore. This is expected because the ionization mechanism then differs too strongly from tunneling, so that rate expressions obtained by modifications of the ADK formula do not provide a suitable description in a far-OBI regime. Instead, the rate dependence has been found to change qualitatively. For OBI of hydrogen

Table 2. Optimized parameters to fit the far-OBI rate to the analytical form given in equation (16).

	a	b	c	d
Hydrogen	2.12 576	2.27 298	0.39 435	1.44 093
Helium	1.11 521	3.46 003	0.35 354	2.23 355

in the range $0.15 \leqslant F/F_a \leqslant 0.5$, an approximately quadratic field dependence

$$W_{\mathrm{OBI}}^{(\mathrm{BM})} \approx 2.4F^2 \tag{14}$$

was obtained by Bauer and Mulser through fitting to ionization rates from a fully numerical solution of the Schrödinger equation [6]. For even higher fields up to about $4F_c$ their numerical results indicated a flattening of the quadratic dependence. Based on a so-called motionless approximation, Kostyukov and Golovanov have predicted a linear increase of the rate [15], according to

$$W_{\mathrm{OBI}}^{(\mathrm{KG})} \approx 0.8F. \tag{15}$$

This formula is supposed to be applicable for $F \gg 3F_c$, reaching up to few times the atomic field F_a. Concerning an approximately linear scaling of OBI rates with the applied field, we also refer to the consideration in [30].

Guided by these findings, we propose the following functional form to model the ionization rate in the far-OBI regime:

$$W_{\mathrm{fOBI}} = \frac{aF^b}{c + F^d}. \tag{16}$$

It contains four fit parameters that will be adjusted to existing numerical OBI rates. The form of equation (16) implies that, for $b \approx 2$ and $d \approx 1$, the field dependence of the rate resembles the quadratic scaling of equation (14) for moderate OBI field strengths, while for very large fields it approaches approximately to a linear growth as in equation (15). We emphasize that, beyond these desirable mathematical properties, we are not aware of an intuitive physical motivation for the form of the far-OBI expression (16), in contrast to our near-OBI treatment in section 2.

In order to determine the fit parameters for hydrogen, we use the predictions from the empirical formula (4) by Zhang *et al* for $F = 3.5F_c$ and $4F_c$, and the numerical rates computed by Bauer and Mulser for higher field strengths $0.6 \lesssim F/F_a \lesssim 4$ (see figure 6 in [6]). As a result, we obtain the values provided in table 2. Accordingly, for moderate field strengths of $F \approx 0.3F_a$ and below, the rate (16) approximately scales as $W_{\mathrm{fOBI}} \sim F^{b_{\mathrm{H}}} \approx F^{2.27}$, resembling the quadratic dependence of equation (14). For large fields $F \gtrsim F_a$ one obtains instead a nearly linear rate growth $W_{\mathrm{fOBI}} \sim F^{b_{\mathrm{H}} - d_{\mathrm{H}}} \approx F^{0.83}$ like in equation (15).

Our prediction for the OBI rate of hydrogen is shown by the solid black curve in figure 6. The curve represents the piecewise defined function

$$W_{\mathrm{OBI}} = \begin{cases} W_{\mathrm{nOBI}}^{(\mathrm{fit})} & \text{for } F \leqslant F_{\mathrm{tr}} \\ W_{\mathrm{fOBI}} & \text{for } F > F_{\mathrm{tr}} \end{cases} \tag{17}$$

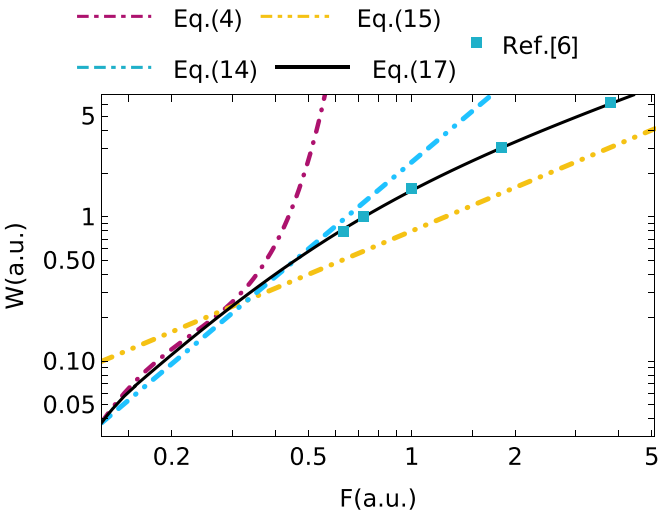

Figure 6. OBI rates for atomic hydrogen in a wide range of field strengths, including the far-OBI regime. The solid black line shows our combined rate formula (17). For comparison, the double-dash-double-dotted cyan line is the quadratic rate (14) by Bauer and Mulser, that was obtained in the range $0.15\,\mathrm{a.u.} \leqslant F \leqslant 0.5\,\mathrm{a.u.}$; the cyan squares at higher field strengths are read off from figure 6 in [6]. The dash-double-dotted yellow line is the linear rate (15) predicted by Kostyukov and Golovanov [15], whereas the dash-dotted purple line is the rate (4) by Zhang *et al* [14].

which combines equation (13) with equation (16) and, thus, extends from the near-OBI to the far-OBI regime. The 'transition field strength' in case of hydrogen is chosen as $F_{\mathrm{tr}} = 2.5F_c$, since equation (13) works well up to this point (see figure 3). For $F \geqslant 2.5F_c \approx 0.16$ a.u., the curve is obtained from equation (16) with the fit parameters given in table 2. It runs very closely to the empirical rate of Zhang *et al* (dash-dotted purple curve) up to $F \approx 0.3$ a.u. and to the rate formula (14) of Bauer and Mulser up to $F \approx 0.5$ a.u. Our rate prediction also matches well the numerical data of Bauer and Mulser (cyan marker points) at higher fields, where their quadratic rate formula (14) starts to deviate. In this region, our rate runs almost parallely to—but significantly higher than—the result of equation (15) by Kostyukov and Golovanov. Overall, the combined formula (17) accomplishes very satisfactory OBI rate predictions in a broad range of field strengths.

Our results from equation (17) for OBI of helium are shown by the black solid curve in figure 7. Here, we take the transition point between near-OBI and far-OBI at $F_{\mathrm{tr}} = 2.05F_c \approx 0.42$ a.u., in accordance with figure 5. The fit parameters entering W_{fOBI} are listed in table 2; they have been obtained based on the numerical results of Scrinzi *et al* [7]. Our corresponding analytical rate prediction of the form (16) reaches very good agreement with these 'exact' numerical data in the full range of considered field strengths. For very large fields $F > 1$ a.u., the rate $W_{\mathrm{fOBI}} \sim F^{b_{\mathrm{He}} - d_{\mathrm{He}}} \approx F^{1.23}$ scales approximately linearly, in accordance with equation (15). However, for helium the rate grows slightly faster than linearly, whereas for hydrogen a slightly sub-linear growth $\sim F^{0.83}$ was obtained above. In an intermediate regime of field strengths around $F \sim 0.5$ a.u. (i.e. $1.8 \lesssim F/F_c \lesssim 3$), the rate increases like $W_{\mathrm{fOBI}} \sim F^{2.66}$ for

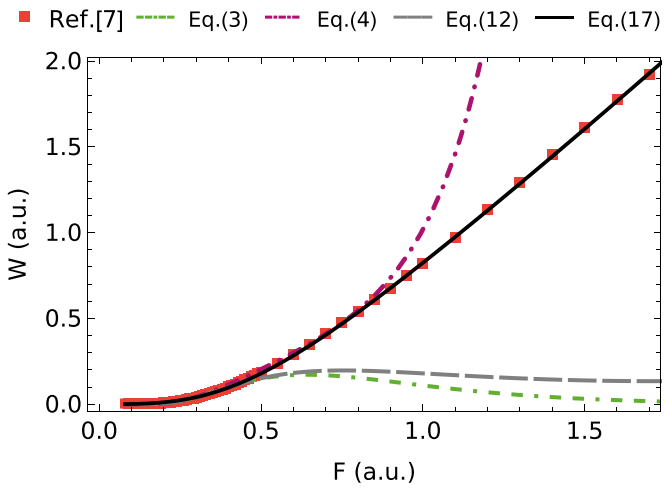

Figure 7. OBI rates for helium, spanning the range from near- to far-OBI. The black solid curve shows our combined rate formula (17), while the red marker squares are the numerical results from Scrinzi *et al* [7]. For comparison, the dash-dotted purple line is the rate (4) by Zhang *et al,* the dash-dotted green curve is the rate (3) by Tong and Lin, whereas the long-dashed gray rate refers to our near-OBI formula (12), which is applicable up to $F \approx 2.05F_c \approx 0.42$ a.u.

helium. Also here the growth is steeper than the one found for hydrogen.

We point out that the static ionization rate $W_{\mathrm{OBI}}(F)$ in the presence of a constant electric field given by equation (17) can be used, under suitable conditions, to calculate the ionization probability of an atom in a time-dependent electric field $F(t)$ (e.g. an oscillating laser pulse in dipole approximation). If the latter exists during the time interval $0 \leqslant t \leqslant T$, the associated ionization probability is approximately obtained as (see. e.g. [8, 14, 19])

$$P_{\mathrm{OBI}} = 1 - \exp\left(-\int_0^T W_{\mathrm{OBI}}\left(|F(t)|\right) \mathrm{d}t\right). \tag{18}$$

This formula applies to slowly varying fields where the time scale of the ionization event is much shorter than the oscillation period of the field, so that the ionization proceeds in a quasi-static manner. When the value of the time-integrated rate is much smaller than one, this expression simplifies to $P_{\mathrm{OBI}} \approx \int_0^T W_{\mathrm{OBI}}\left(|F(t)|\right) \mathrm{d}t$.

4. Aspects beyond atomic physics

4.1. Application in plasma simulation codes

Analytical rate formulas for strong-field ionization are useful as elementary building blocks in numerical codes for simulation of the many-body dynamics in laser-generated plasmas. Early implementations in particle-in-cell codes relied on the ADK formula solely (see, e.g. [31–33]). In more recent years, this approach has been extended in order to properly account for ionization in the OBI regime as well. To this end, piecewise combinations of the ADK formula with the far-OBI rates (14) and/or (15) have been implemented [34, 35]. These rate formulas are 'glued together' at their crossing points to obtain a continuous field dependence. Also the near-OBI rate (3) of Tong and Lin is applied in particle-in-cell codes [36].

However, the various implementations of analytical field ionization rates presently in use can lead to different numerical outcomes, as has been analyzed recently [37]. This happens when the rate formulas are extended beyond their range of applicability. For example, the tunneling-like near-OBI formula (3) of Tong and Lin underestimates the ionization rate for $F \gtrsim 2.5F_c$, while the linear far-OBI formula (15) by Kostyukov and Golovanov underestimates the rate for $F > F_a$.

This situation can be improved by the piecewise combined rate formula in equation (17). It offers the advantage to achieve not only a smooth transition from the tunneling regime to the near-OBI domain of Tong and Lin to the quadratic far-OBI region of Bauer and Mulser and eventually to the linear far-OBI regime, but is additionally in close agreement with fully numerical data. Accordingly, our combined rate overcomes the difficulties addressed in [37] and can, thus, be useful for application in large-scale plasma simulation codes.

4.2. Relation to strong-field pair production

The transition of the ionization rate from the tunneling to the near- and far-OBI regimes has a close analogy in other strong-field phenomena. For example, in the strong-field Breit-Wheeler process, electron–positron pairs are created from vacuum by a high-energy γ-photon of frequency ω' colliding with an intense laser field [38]. In the regime of high laser intensities, where the quantum nonlinearity parameter $\chi \sim \omega' F/F_{\mathrm{cr}} \ll 1$ is still small, the pair production rate $W_{\mathrm{BW}} \sim \mathrm{e}^{-8/(3\chi)}$ has a tunneling-like form, very similar to equation (1). Here $F_{\mathrm{cr}} = c_0^3$ denotes the critical field strength of quantum electrodynamics, with the speed of light $c_0 = 137$ a.u. in vacuum. The tunneling rate formula continues to hold approximately in the intermediate 'near over-barrier' region of $\chi \sim 1$, but overestimates the exact result (see, e.g. figure 5 in [39]). Eventually, in the 'far over-barrier' regime for $\chi \gg 1$, the field dependence of the rate changes into a fractional power-law of the form $W_{\mathrm{BW}} \sim F^{2/3}$. In case of the strong-field Bethe-Heitler process, that is electron–positron pair production in combined Coulomb and laser fields, the exponential tunneling-like rate transitions to an $W_{\mathrm{BH}} \sim F\ln(F)$ dependence in the far over-barrier regime [40]. Hence, strong-field ionization and pair production share qualitatively similar, though not identical nonperturbative features.

5. Conclusion

OBI of hydrogen and helium atoms has been studied on the basis of phenomenological rate formulas. It was shown that the successful analytical rate expressions by Tong and Lin [8] and by Zhang *et al* [14] for ionization in a near-OBI regime can be physically interpreted as arising from modifications of the ADK tunneling rate by the Stark effect and a widened range of electron emission angles. Our corresponding approach provides ionization rates that are in close agreement with these established empirical formulas and with fully numerical results for hydrogen and helium.

We emphasize that our considerations were purely phenomenologically oriented and, consequently, do not represent rigorous derivations. They may thus be regarded complementary to a recent thorough treatment of (relativistic) strong-field ionization and OBI [16]. Both considerations have in common that they account for the Stark energy shift and the distortion of the atomic bound state. However, in [16] these effects are incorporated directly in the electron wave function, whereas we have included them at the level of the ionization rate. The ejected electron is affected in very different ways by either including the atomic potential perturbatively in the continuum state [16], or a widened angular emission range.

In the far-OBI regime of very large (but still nonrelativistic) field strengths we have presented compact four-parameter rate formulas that agree very well with available numerical data and generalize analytical expressions obtained previously by Bauer and Mulser [6] and by Kostyukov and Golovanov [15]. Our near-OBI and far-OBI rate formulas can be joined to cover a very broad range of field strengths. The resulting analytical expression can be implemented in large-scale laser-plasma codes to describe elementary ionization events.

Data availability statement

All data that support the findings of this study are included within the article (and any supplementary files).

ORCID iDs

A B Voitkiv 0000-0003-1420-5915
C Müller 0009-0008-9123-2662

References

[1] Fedorov M V 1997 *Atomic and Free Electrons in a Strong Light Field* (World Scientific)
Milošević D B, Paulus G G, Bauer D and Becker W 2006 *J. Phys. B: At. Mol. Opt. Phys.* **39** R203
Grossmann F 2008 *Theoretical Femtosecond Physics: Atoms and Molecules in Strong Laser Fields* (Springer)
[2] Agostini P and DiMauro L F 2004 *Rep. Prog. Phys.* **67** 813
Scrinzi A, Ivanov M Y, Kienberger R and Villeneuve D M 2006 *J. Phys. B: At. Mol. Opt. Phys.* **39** R1
Winterfeldt C, Spielmann C and Gerber G 2008 *Rev. Mod. Phys.* **80** 117
[3] Hidding B, Pretzler G, Rosenzweig J B, Königstein T, Schiller D and Bruhwiler D L 2012 *Phys. Rev. Lett.* **108** 035001
Deng A *et al* 2019 *Nat. Phys.* **15** 1156
[4] Ammosov M V, Delone N B and Krainov V P 1987 *Sov. Phys. JETP* **64** 1191
[5] Perelomov A M, Popov V S and Terentev M V 1966 *Sov. Phys. JETP* **23** 924
Perelomov A M and Popov V S 1967 *Sov. Phys. JETP* **25** 336
[6] Bauer D and Mulser P 1999 *Phys. Rev. A* **59** 569
[7] Scrinzi A, Geissler M and Brabec T 1999 *Phys. Rev. Lett.* **83** 706
[8] Tong X M and Lin C D 2005 *J. Phys. B: At. Mol. Opt. Phys.* **38** 2593
[9] Lötstedt E, Ciappina M F and Yamanouchi K 2020 *Phys. Rev. A* **102** 013112
[10] Jones E C, Andreula Z P and Walker B C 2023 *Phys. Rev. A* **107** 033102
[11] Posthumus J H, Thompson M R, Frasinski L F and Codling K 1997 *Multiphoton Processes 1996* (*IOP Conference Series*) Proc. No. 154 (Institute of Physics and Physical Society) ed P Lambropoulos and H Walther p 298
[12] Delone N B and Krainov V P 1998 *Phys.-Usp.* **41** 469 (see equation (48) therein)
[13] The electron dynamics during OBI has very recently been studied in Ma Y, Liu Q, Ni H and Wu J 2025 (arXiv:2509.02026)
[14] Zhang Q, Lan P and Lu P 2014 *Phys. Rev. A* **90** 043410
[15] Kostyukov I Y and Golovanov A A 2018 *Phys. Rev. A* **98** 043407
[16] Klaiber M, Hatsagortsyan K Z and Keitel C H 2024 *Phys. Rev. A* **110** 023103
[17] Ivanov I A and Ho Y K 2004 *Phys. Rev. A* **69** 023407
[18] Maltsev I A, Tumako D A, Popov R V and Shabaev V M 2022 *Opt. Spectrosc.* **130** 455
[19] A pedagogical derivation of the ADK rate is given in Bisgaard C Z and Madsen L B 2004 *Am. J. Phys.* **72** 249
[20] Equation (2) represents the standard formula for the over-barrier threshold field and results from a one-dimensional consideration. A more sophisticated treatment, which also accounts for the lateral electron motion, leads to a larger value of $(\sqrt{2}-1)I_p^{3/2} \approx 0.146$ a.u. in case of hydrogen, due to its special symmetry; see Bauer D 1997 *Phys. Rev. A* **55** 2180
[21] As pointed out in [15], a misprinted minus sign needs to be fixed in the exponent of equation (8) in [14].
[22] Akagi H, Otobe T, Staudte A, Shiner A, Turner F, Dörner R, Villeneuve D M and Corkum P B 2009 *Science* **325** 1364
[23] Holmegaard L *et al* 2010 *Nat. Phys.* **6** 428
[24] Trinh V H, Tolstikhin O I, Madsen L B and Morishita T 2013 *Phys. Rev. A* **87** 043426
[25] Landau L D and Lifshitz E M 1965 *Quantum Mechanics* (Sec 77) (Oxford)
[26] Dimitrovski D *et al* 2011 *Phys. Rev. A* **83** 023405
Hansen J L *et al* 2011 *Phys. Rev. A* **83** 023406
[27] Damburg R J and Kolosov V V 1978 *J. Phys. B* **11** 1921 (see equation (47) therein)
[28] Tong X M, Zhao Z X and Lin C D 2002 *Phys. Rev. A* **66** 033402
[29] This Stark shift is in close accordance with the results for the helium polarizability at low field strengths obtained in Gründler W, Steinke T and Walther P 1990 *J. Comput. Chem.* **11** 548
[30] Popov V S 2000 *J. Exp. Theor. Phys.* **91** 48
[31] Bruhwiler D L, Dimitrov D A, Cary J R, Esarey E, Leemans W and Giacone R E 2003 *Phys. Plasmas* **10** 2022
[32] Nuter R, Gremillet L, Lefebvre E, Lévy A, Ceccotti T and Martin P 2011 *Phys. Plasmas* **18** 033107
[33] Chen M, Cormier-Michel E, Geddes C G R, Bruhwiler D L, Yu L L, Esarey E, Schroeder C B and Leemans W P 2013 *J. Comput. Phys.* **236** 220
[34] Artemenko I I and Kostyukov I Y 2017 *Phys. Rev. A* **96** 032106
[35] Ouatu I *et al* 2022 *Phys. Rev. E* **106** 015205
[36] Derouillat J *et al* 2018 *Comput. Phys. Commun.* **222** 351
[37] Mironov A A *et al* arXiv:2501.11672
[38] Ritus V I 1985 *J. Sov. Laser Res.* **6** 497
[39] Golub A, Villalba-Chávez S and Müller C 2022 *Phys. Rev. D* **105** 116016
[40] Yakovlev V P 1966 *Sov. Phys. JETP* **22** 223
Milstein A I, Müller C, Hatsagortsyan K Z, Jentschura U D and Keitel C H 2006 *Phys. Rev. A* **73** 062106